NIR-mbc94, a Fluorescent Ligand that Binds to Endogenous CB$_2$ Receptors and Is Amenable to High-Throughput Screening

Michelle Sexton[1], **Grace Woodruff**[2], **Eric A. Horne**[1], **Yi Hsing Lin**[1], **Giulio G. Muccioli**[3], **Mingfeng Bai**[4], **Eric Stern**[5], **Darryl J. Bornhop**[5], and **Nephi Stella**[1,6,*]

[1]Department of Pharmacology, University of Washington, Seattle, WA 98195-7280, USA

[2]Neurobiology Undergraduate Program, University of Washington, Seattle, WA 98195-7280, USA

[3]Bioanalysis and Pharmacology of Bioactive Lipids Laboratory, CHAM7230, Louvain Drug Research Institute, Université Catholique de Louvain, Av. E. Mounier 72, B-1200, Bruxelles B-1200, Belgium

[4]Department of Radiology, University of Pittsburg Medical Center, Pittsburg, PA 15219, USA

[5]Department of Chemistry and the Vanderbilt Institute of Chemical Biology, Vanderbilt University, Nashville, TN 37235-1822, USA

[6]Psychiatry and Behavioral Sciences, University of Washington, Seattle, WA 98195-7280, USA

SUMMARY

High-throughput screening (HTS) of chemical libraries is often used for the unbiased identification of compounds interacting with G protein-coupled receptors (GPCRs), the largest family of therapeutic targets. However, current HTS methods require removing GPCRs from their native environment, which modifies their pharmacodynamic properties and biases the screen toward false positive hits. Here, we developed and validated a molecular imaging (MI) agent, NIR-mbc94, which emits near infrared (NIR) light and selectively binds to endogenously expressed cannabinoid CB$_2$ receptors, a recognized target for treating autoimmune diseases, chronic pain and cancer. The precision and ease of this assay allows for the HTS of compounds interacting with CB$_2$ receptors expressed in their native environment.

INTRODUCTION

GPCRs represent the largest family of proteins targeted for therapeutic benefit (Lagerstrom and Schioth, 2008). Numerous analytical methods have been developed to determine the molecular details of ligands interacting with GPCRs. Some of these analytical methods were miniaturized and formatted for the HTS of chemical libraries, and were successfully used for the unbiased identification of hits, followed by their optimization toward lead compounds and drug candidates. Examples include fluorescent polarization and biosensors, such as CellKey and the SRU BIND system, which monitor the direct interaction of compounds with GPCRs (Ciambrone et al., 2004; Cunningham et al., 2004; Leopoldo et al., 2009). Another example is the coexpression of GPCRs with promiscuous G$_{\alpha 15/16}$ proteins, which monitors ligand-induced regulation of signal transduction pathways (Kostenis et al., 2005).

While these approaches are excellent at screening large numbers of compounds, they have limitations. For example, fluorescence polarization requires receptors that are removed from their native environment (because it requires isolation of the protein in aqueous solution). Biosensors depend on indirect signaling. Promiscuous coupling of GPCRs to $G_{\alpha 15/16}$ requires the heterologous expression of the target receptor and this particular effector protein: $G_{\alpha 15/16}$. This introduces unwarranted interactions between proteins endogenously expressed by the host cell and the target and its effector protein complex. All these limitations can affect the pharmaco-dynamic properties and coupling efficacy of the targeted GPCR, and thus bias the HTS toward false positive hits. In fact, restricting the number of hits resulting from a HTS to those that represent true interactions with the targeted GPCR is extremely important for drug development, because validating and optimizing each hit represents an enormous endeavor. Considering this notion, attention has been dedicated to the development of analytical methods allowing for the HTS of compounds at GPCRs that are endogenously expressed by cells, which cuts down the number of false-positive hits.

Molecular imaging (MI) provides a versatile approach for investigating dynamic molecular events (Du et al., 2006). Typically, MI agents are high-affinity ligands (small molecules, antibodies, peptides, carbohydrates or enzyme substrates) conjugated to a biocompatible imaging moiety, and allow for the real-time visualization of changes in the expression or activities of the targeted receptor or enzyme. Thus, MI agents can be used as diagnostic tools, as they allow one to follow the fluctuations in the expression and activity of a relevant receptor or enzyme as a function of disease progression or therapeutic intervention (Achilefu, 2010; Banati, 2003). Examples of MI agents that target receptors with diagnostic and therapeutic value include agents that bind to the endothelial growth factor receptor, a receptor tyrosine kinase involved in cancer pathogenesis, and agents that bind to the somatostatin receptors 5, a GPCR involved in psychiatric disorders (Diagaradjane et al., 2008; Edwards et al., 2008). While these MI agents are excellent at following the fluctuations in the expression and activity of these targets endogenously expressed by native cells, they are not fit for miniaturization and formatting for HTS because of their limited detectable and quantifiable emission spectra.

Because of its recognized therapeutic value, we chose to develop a MI agent that binds to CB_2 receptors (Buckley, 2008; Thakur et al., 2009). Our goal was threefold: (1) validate the binding of this MI agent to endogenously expressed CB_2 receptors, (2) optimize the detection of the signal emitted by this interaction, and (3) format and validate the assay for HTS. CB_2 receptors couple to $G_{i/o}$ proteins and are expressed by immune cells and some tumor cells (Stella, 2010). Activation of CB_2 receptors expressed by immune cells reduces the production of immune modulators and regulates immune cell migration; thus, compounds interacting with this target have therapeutic value for immune-related diseases (Stella, 2009). Activation of CB_2 receptors expressed by malignant cells also regulates their cell migration, but in this case activates apoptosis and thus kills malignant cells, making agonists at CB_2 receptors promising therapeutic agents (Fernandez-Ruiz et al., 2007; Guzmán, 2003). Thus, MI agents that bind to CB_2 receptors would constitute useful chemical tools to develop novel therapeutics.

RESULTS

SR144528 is a selective inverse agonist that exhibits nanomolar affinity at CB_2 receptors (Rinaldi-Carmona et al., 1998). While SR144528 represents an interesting chemical scaffold to develop MI agents that bind to CB_2 receptor, it lacks the functional groups that allow for the easy bioconjugation of linkers and imaging moieties. Thus, in a first set of experiments, we developed new synthesis schemes that introduce an amino group in SR144528, making it suitable for bioconjugations (Bai et al., 2008). Another challenge was that no data on the

structure-activity relationship (SAR) of SR144528 binding to CB_2 receptors is available. To circumvent this issue, we (1) synthesized three SR144528 analogs that contained primary amino groups in strategic positions, (2) coupled each amino group to 1,6-diaminohexyl linker arms (Figure 1A; see Figure S1 available online), and (3) tested their ability to outcompete [^{3}H]-CP-55,940 binding to CB_2 receptors. We found that the addition of an alkyl amino chain to the R_3 position decreases the affinity by only 15-fold (Figure 1B), whereas this addition to the C3 position of the pyrazole scaffold (R_1) or to the 4-chloro-3-methylphenyl substituent (R_2) (named ES51 and ES52, respectively) obliterated binding to CB_2 receptors (Figures S2A and S2B). Thus we focused our efforts on R_3-mbc94 and found that its conjugation to the NIR emitting moiety, IRDye 800CW (Ntziachristos et al., 2003), further reduced its affinity at CB_2 receptors by only 17-fold ($Ki = 260$ nM, Figure 1B). These results suggest that NIR-mbc94 is a promising MI agent to monitor CB_2 receptor occupancy and expression.

Next, we verified that NIR-mbc94 binds to CB_2 receptors expressed by intact cells. Indeed, the affinity of a ligand for its target may change drastically when comparing data obtained with cell homogenates versus intact cells (for examples of such discrepancies, see Sexton et al. [2009] and Toll [1995]). Thus, we determined the ability of NIR-mbc94 to bind to intact CB_2- mid DBT cells in culture (i.e., cells heterologously expressing mouse CB_2 receptors at levels that are found in native cells; Cudaback et al., 2010). To measure the fluorescent signal emitted by NIR-mbc94, we used a LI-COR Odyssey scanner, which is suitable for HTS. Note that we optimized the signal-to-noise ratio of this assay by systematically varying several parameters, including cell density, the composition of cell culture media and the time that cells are preincubated with excess unlabeled compounds (data not shown). Using the optimized conditions outlined in the methods sections, we found that NIR-mbc94 binds specifically to intact CB_2-mid DBT cells, an interaction that reached equilibrium in 30 min (data not shown) and was saturable ($Kd = 400$ nM) (Figure 2A). Conversely, NIR-mbc94 did not bind to untransfected DBT cells, which lack endogenous CB_2 receptors (data not shown) (Cudaback et al., 2010). The precision of this assay was such that it allowed for the generation of detailed competition curves. Specifically, both the original chemical scaffold, SR144528, and a structurally distinct CB_2 agonist, WIN55212-2 (WIN), competed for NIR-mbc94 binding at CB_2 receptors ($Ki = 4.7$ nM and 3 nM, respectively) (Figures 2C and 2D). We then performed two sets of experiments to test the versatility of this new MI agent. First, we screened a small library of compounds (1 μM) to determine if NIR-mbc94 can reliably detect a hit among several inactive compounds. Indeed, we reliably detected a reduction in NIR-mbc94 signal when applying compounds that are known to bind to CB_2 receptors (Table S1). Furthermore, the NIR-mbc94 signal remained unperturbed when applying drugs that are inactive at this target (Table S1). Note that this library contained several new scaffolds that significantly reduced the NIR-mbc94 signal, suggesting that these compounds are binding to CB_2 receptors and thus represent hits (Table S1). Second, we used a microscope coupled to a camera that detects NIR light and found that we could reliably visualize NIR-mbc94 bound to CB_2 receptors expressed by intact cells (Figure 2B; Figure S2). Together these data show that NIR-mbc94 binds to CB_2 receptors expressed by intact cells. This interaction is easily and reliably quantified with a detector suitable for HTS and a microscope coupled to a camera that detects NIR light.

To determine if NIR-mbc94 binds to CB_2 receptors endogenously expressed by cells, we used two cell types known to express this target: (1) BV-2 cells, a mouse microglia cell line, and (2) mouse microglia cells in primary culture (Walter et al., 2003). In BV-2 cells, WIN competed for NIR-mbc94 binding ($Ki = 3$ nM) and yielded approximately 60%–70% specific binding (Figure 3A), confirming the fact that these cells express high levels of endogenous CB_2 receptors (Walter et al., 2003). In primary microglia, we found that NIR-mbc94 also binds specifically, although at much lower level, and that its signal increased

when treating the cells with IL-4 (Figure 3B). With regard to this result, two controls are noteworthy. First, using qPCR we found that IL-4 treatment increased CB_2 receptor mRNA in primary microglia by ~5-fold, whereas functionally different cytokines, TNFα + IFNγ and TGFβ, did not affect the expression of this target (Figure S3). This result is noteworthy because IL-4 promotes an alternative activation phenotype in macrophages/microglia (M2 phenotype) and inhibits classical activation (M1 phenotype) (Ponomarev et al., 2007). Second, we obtained the genetic validation of NIR-mbc94's selective binding to $CB_2^{-/-}$ receptors since NIR-mbc94 did not exhibit specific binding when applied to primary microglia generated from CB_2 mice (Figure 3B). Together, these data demonstrate that NIR-mbc94 binds selectively to CB_2 receptors endogenously expressed by intact cells.

DISCUSSION

Developing new tools that allow for the HTS of compounds interacting with GPCRs endogenously expressed by cells constitutes the next state-of-the-art approach for the unbiased identification of therapeutic candidates. Using systematic chemical modifications, we developed a MI agent that selectively interacts with CB_2 receptors endogenously expressed by intact cells. To our knowledge, this MI agent is among the first to reliably measure the occupancy of endogenously expressed receptors using intact cells and a HTS platform for quantification. Detecting the changes in the fluorescence emitted by NIR-mbc94 bound to its target allow for the precise determination of the basic binding constants exhibited by agonist and antagonist at CB_2 receptors. At this point it is unclear whether the high level of nonspecific binding found in primary microglia makes NIR-mbc94 suitable for any in vivo imaging approaches aimed at assessing CB_2 receptor expression or occupancy, a technology that would have clear diagnostic and therapeutic value. Nevertheless, because our experiments were performed on intact cells grown in 96-well plates, which can be easily miniaturized to 384-well plates, and because the emitted fluorescence was detected using a Li-Cor Odyssey scanner, which allows for rapid and linear quantification of fluorescence, the new assay that we report here is amenable to the HTS of chemical libraries. Developing drugs that specifically target CB_2 receptors expressed by immune and tumor cells constitutes a promising therapeutic venue for developing medicine aimed at treating autoimmune diseases, chronic pain and tumors.

SIGNIFICANCE

Cannabinoid CB_2 receptors are G protein-coupled receptors expressed by immune cells and nearly absent in healthy brain parenchyma. Under neuroinflammatory conditions, their expression in microglia, the macrophages of the brain, can increase by as much as 100-fold. This cell specific increase in CB_2 receptor expression makes this protein an ideal target for drugs aimed at regulating neuroinflammation. These receptors are also expressed by tumor cells, and in this case CB_2 receptor agonists induce apoptosis, indicating that such ligands represent promising therapeutic agents.

Here, we report the development and validation of a molecular imaging agent, NIR-mbc94, that selectively binds to CB_2 receptors. NIR-mbc94 was developed by conjugating a high affinity antagonist at CB_2 receptors, SR144528, to a biocompatible fluorophore that emits near infrared light (wavelengths that exhibit minimal tissue absorbance). We provide the genetic validation of NIR-mbc94's selectivity at CB_2 receptors, and demonstrate that it binds to these receptors expressed in their native environment (endogenously expressed by intact cells). The signal emitted by NIR-mbc94 bound to CB_2 receptors, and the ease of the detection of this interaction, allows for the unbiased HTS of compounds interacting with this therapeutic target.

EXPERIMENTAL PROCEDURES

Chemicals

CellGro was purchased from Mediatech (Washington DC) and DRAQ5 from Axxora (San Diego, CA). [^{3}H]-CP-55, 940, CP-55,940, SR144528 and WIN55212-2 were from the NIDA drug supply system.

Synthesis of NIR-mbc94

Three variations of a conjugable version of SR144528 were synthesized with a hexane-1,6-diamine linker at three different positions: In short, a high yield (84%) method was described previously with regular peptide coupling, followed by *N*-alkylation at positions R1, R2, and R3. Subsequently in a facile DMSO reaction, we added IRDye 800CW NHS ester, then purified via HPLC and characterized by NMR and mass spectrometry. We then further confirmed that absorption and emission spectra of the dye were not altered by conjugation to the ligand (Bai et al., 2008). Analogs R1 and R2 were coupled to the NIR-Dye and purified using the same pathway. The differences are the synthetic pathways to obtain the halogenated precursors (unpublished data).

Cells in Culture

DBT CB$_2$-mid cells are mouse delayed brain tumor (DBT) cells heterologously expressing mouse CB$_2$ receptors at levels that lie well within the range of this receptor's endogenous levels in various cell lines (Cudaback et al., 2010). These cells were generated and expanded as previously described (Cudaback et al., 2010). BV-2 cells in culture were expanded as previously described (Walter et al., 2003). Mouse microglia in primary culture from wild-type and CB$_2^{-/-}$ pups were prepared as described (Walter et al., 2003), according to the guidelines of the Institutional Animal Care and Use committee of the University of Washington.

Radioligand Binding

CB$_2$-mid DBT cells were grown to confluence in 10 mm culture dishes and homogenates containing their enriched membranes prepared as follow: cells were rinsed once with PBS, frozen, lysed in Tris-EDTA-MgCl$_2$ buffer (50 mM, 1 mM, 3 mM [pH 7.4]; buffer A), homogenized using a polytron homogenizer and the resulting homogenate centrifuged (20 min at 14,000 × g, 4°C). Supernatant was discarded and pellets resuspended using the same buffer, and centrifuged at 14,000 × g (20 min, 4°C). Saturations and binding experiments were performed using silanized tubes and silanized pipettes tips. Homogenates (50 μg of protein in 150 μl of buffer A containing 1% fatty acid free-BSA) were added to tubes containing either 0.2 μl of drug in DMSO or DMSO alone (0.1%, total binding) and 50 μl of [^{3}H]-CP-55,940 (~3 nM final concentration). Non-specific binding was determined in the presence of 10 μM CP-55,940. Tubes were incubated for 1 hr in a shaking water bath at 30°C. Cold buffer was rapidly added to the tubes, solutions filtered through presoaked glass-fiber filters (Whatman GF/B) using a Brandell harvester (Gaithersburg, MD) and tubes rinsed twice using cold buffer. Radioactivity on the filter was counted using 10 ml of Ecoscint scintillation liquid following 10 sec of agitation and 3 hr resting prior to scintillation counting (PerkinElmer, Boston, MA). *Ki* values were calculated from the IC$_{50}$ values using the Cheng-Prusoff equation. Under these conditions, the B$_{max}$ and K$_d$ values for [^{3}H]-CP-55,940 were 6 pmol/mg and 3.1 nM, respectively (data not shown).

Live Cell Imaging

CB$_2$-mid DBT cells were grown in 6-well plates with optical bottom. Twenty-four hours later, we labeled the nuclei with DRAQ5 (700 nM, 15 min at 37°C). Cells were then labeled

with 1 μM NIR-mbc94 for 20 min (with or without preincubation with 150 nM WIN55212-2 for 15 min at 37°C). Each well was then rinsed twice with DMEM supplemented with 1% BSA and immediately imaged. Fluorescent images were collected on a Zeiss Axio Observer Z1 with a Pan-Apochromatic 63×/1.4 oil lens using Hamamatsu Orca512G camera. The NIR fluorescence of NIR-mbc94 was imaged using Chroma 41037 Li-Cor for IR Dye 800 filter cube. Images were collected with the same exposure settings as unlabeled untransfected DBT cell controls. Background fluorescence was set at the signal emitted by NIR-mbc94 in the presence of 150 nM WIN55212-2 (Figure S2). Data were collected using Axiovision 4.7 software. Images were processed in Adobe Photoshop by gating the background to the untransfected DBT cells as controls followed by setting the intensity to the experimental sample.

Binding in Intact Cells

We used 96-well plates with optical bottom polymer (NUNC). For CB_2-mid DBT cells, each well was previously coated with collagen (2.5 mg/ml), and cells were plated at 40,000 cells in 100 μl of DMEM + 10% FBS per well. For BV-2 cells and microglia in primary culture, each well was coated with poly-ornithine 0.1 mg/ml and cells were plated at 40,000 cells in 100 μl of MEM + Cell Gro (10%) per well. Twenty-four hours later, cells reached ~80% confluence and were preincubated for 15 min with increasing concentrations of drug or vehicle (0.1% DMSO), followed by an incubation with NIR-mbc94 (200 nM, 30 min for CB_2-mid DBT cells, and 1 hr for BV-2 cells and microglia in primary culture). One rinse with MEM/1% FBS stopped the incubation. Fluorescence was immediately measured with a Li-Cor Odyssey Infrared Imaging System using the 800 nm channel (intensity of 4 and focus offset of 3).

qPCR

Microglia in primary cultures were plated in MEM/10% Cellgro at a density of 50,000 cells per well (24-well plates) and labeled with dye as described above. IL-4 (10 ng/ml), TNFα (5 ng/ml) + IFNγ (100 IU/ml), TGFβ (1 μg/ml), or vehicle control was added directly to the cell culture media. After 72 hr, the media was removed, and cells were frozen. RNA was then extracted using RNeasy micro kit (QIAGEN). Real-time quantitative PCR assays were performed using the Brilliant® II QRT-PCR Master Mix, 1-Step kit (Stratagene). Probes for CB_2 were obtained from Roche Applied Science (Universal Probe Library Set, #84,) and HPRT (housekeeping gene) from Applied Biosystems. Primer sequences for the CB_2 mRNA are 5′ tcctatcatttacgccctgc 3′ and 5′ ggctccta ggtggttttcacatcagcctc 3′; and for the hprt mRNA are: 5′cctaagatgagcgca agttgaa3′ and 5′ ccacaggactagaacacctgctaa3′. Amplifications were run using a Stratagene Mx3000P QPCR system and consisted of 30 min incubation at 45°C, followed by a 10 min denaturation at 95°C and 40 cycles of 1 min at 95°C and 30 sec at 60°C.

Calculations and Statistical Analysis

Data are expressed as n = number of determinations (three per independent experiment). Statistical analysis, *Kd* and *Ki* values (calculated by nonlinear regression) were calculated using GraphPad Prism 4 (San Diego, CA). For specific binding, the values for nonspecific binding were subtracted from total binding values.

Supplementary Material

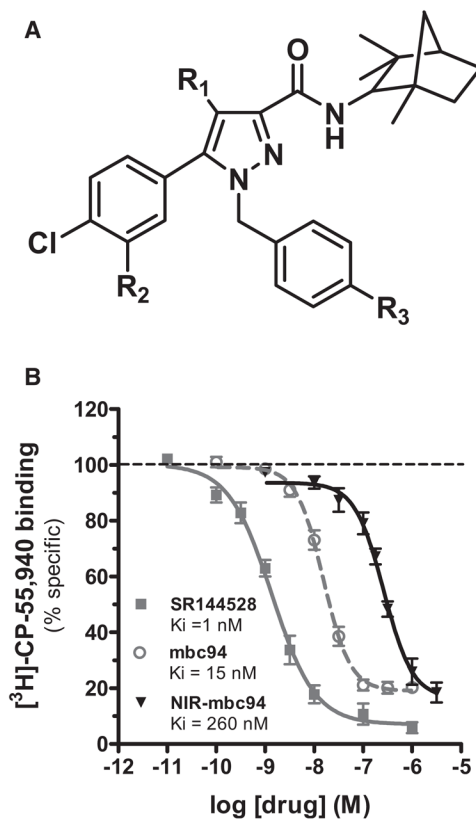Refer to Web version on PubMed Central for supplementary material.

Acknowledgments

References

Achilefu S. Introduction to concepts and strategies for molecular imaging. Chem Rev. 2010; 110:2575–2578. [PubMed: 20415501]

Bai M, Sexton M, Stella N, Bornhop DJ. MBC94, a conjugable ligand for cannabinoid CB 2 receptor imaging. Bioconjug Chem. 2008; 19:988–992. [PubMed: 18444670]

Banati RB. Neuropathological imaging: in vivo detection of glial activation as a measure of disease and adaptive change in the brain. Br Med Bull. 2003; 65:121–131. [PubMed: 12697620]

Buckley NE. The peripheral cannabinoid receptor knockout mice: an update. Br J Pharmacol. 2008; 153:309–318. [PubMed: 17965741]

Ciambrone GJ, Liu VF, Lin DC, McGuinness RP, Leung GK, Pitchford S. Cellular dielectric spectroscopy: a powerful new approach to label-free cellular analysis. J Biomol Screen. 2004; 9:467–480. [PubMed: 15452333]

Cudaback E, Marrs W, Moeller T, Stella N. The expression level of CB1 and CB2 receptors determines their efficacy at inducing apoptosis in astrocytomas. PLoS ONE. 2010; 5:e8702. [PubMed: 20090845]

Cunningham BT, Li P, Schulz S, Lin B, Baird C, Gerstenmaier J, Genick C, Wang F, Fine E, Laing L. Label-free assays on the BIND system. J Biomol Screen. 2004; 9:481–490. [PubMed: 15452334]

Diagaradjane P, Orenstein-Cardona JM, Colon-Casasnovas NE, Deorukhkar A, Shentu S, Kuno N, Schwartz DL, Gelovani JG, Krishnan S. Imaging epidermal growth factor receptor expression in vivo: pharmacokinetic and biodistribution characterization of a bioconjugated quantum dot nanoprobe. Clin Cancer Res. 2008; 14:731–741. [PubMed: 18245533]

Du W, Wang Y, Luo Q, Liu BF. Optical molecular imaging for systems biology: from molecule to organism. Anal Bioanal Chem. 2006; 386:444–457. [PubMed: 16850295]

Edwards WB, Xu B, Akers W, Cheney PP, Liang K, Rogers BE, Anderson CJ, Achilefu S. Agonist-antagonist dilemma in molecular imaging: evaluation of a monomolecular multimodal imaging agent for the somatostatin receptor. Bioconjug Chem. 2008; 19:192–200. [PubMed: 18020401]

Fernandez-Ruiz J, Romero J, Velasco G, Tolon RM, Ramos JA, Guzman M. Cannabinoid CB2 receptor: a new target for controlling neural cell survival? Trends Pharmacol Sci. 2007; 28:39–45. [PubMed: 17141334]

Guzmán M. Cannabinoids: potential anticancer agents. Nat Rev Cancer. 2003; 3:745–755. [PubMed: 14570037]

Kostenis E, Waelbroeck M, Milligan G. Techniques: promiscuous Galpha proteins in basic research and drug discovery. Trends Pharmacol Sci. 2005; 26:595–602. [PubMed: 16183138]

Lagerstrom MC, Schioth HB. Structural diversity of G protein-coupled receptors and significance for drug discovery. Nat Rev Drug Discov. 2008; 7:339–357. [PubMed: 18382464]

Leopoldo M, Lacivita E, Berardi F, Perrone R. Developments in fluorescent probes for receptor research. Drug Discov Today. 2009; 14:706–712. [PubMed: 19573791]

Ntziachristos V, Bremer C, Weissleder R. Fluorescence imaging with near-infrared light: new technological advances that enable in vivo molecular imaging. Eur Radiol. 2003; 13:195–208. [PubMed: 12541130]

Ponomarev ED, Maresz K, Tan Y, Dittel BN. CNS-derived interleukin-4 is essential for the regulation of autoimmune inflammation and induces a state of alternative activation in microglial cells. J Neurosci. 2007; 27:10714–10721. [PubMed: 17913905]

Rinaldi-Carmona M, Barth F, Millan J, Derocq JM, Casellas P, Congy C, Oustric D, Sarran M, Bouaboula M, Calandra B, et al. SR 144528, the first potent and selective antagonist of the CB2 cannabinoid receptor. J Pharmacol Exp Ther. 1998; 284:644–650. [PubMed: 9454810]

Sexton M, Woodruff G, Cudaback E, Kreitzer FR, Xu C, Lin YH, Moller T, Bai M, Manning HC, Bornhop D, et al. Binding of NIR-conPK and NIR-6T to astrocytomas and microglial cells: evidence for a protein related to TSPO. PLoS ONE. 2009; 4:e8271. [PubMed: 20020060]

Stella N. Endocannabinoid signaling in microglial cells. Neuropharm. 2009; 56(Suppl 1):244–253.

Stella N. Cannabinoid and cannabinoid-like receptors in microglia, astrocytes, and astrocytomas. Glia. 2010; 58:1017–1030. [PubMed: 20468046]

Thakur GA, Tichkule R, Bajaj S, Makriyannis A. Latest advances in cannabinoid receptor agonists. Expert Opin Ther Pat. 2009; 19:1647–1673. [PubMed: 19939187]

Toll L. Intact cell binding and the relation to opioid activities in SH-SY5Y cells. J Pharmacol Exp Ther. 1995; 273:721–727. [PubMed: 7752076]

Walter L, Franklin A, Witting A, Wade C, Xie Y, Kunos G, Mackie K, Stella N. Non-psychotropic cannabinoid receptors regulate microglial cell migration. J Neurosci. 2003; 23:1398–1405. [PubMed: 12598628]
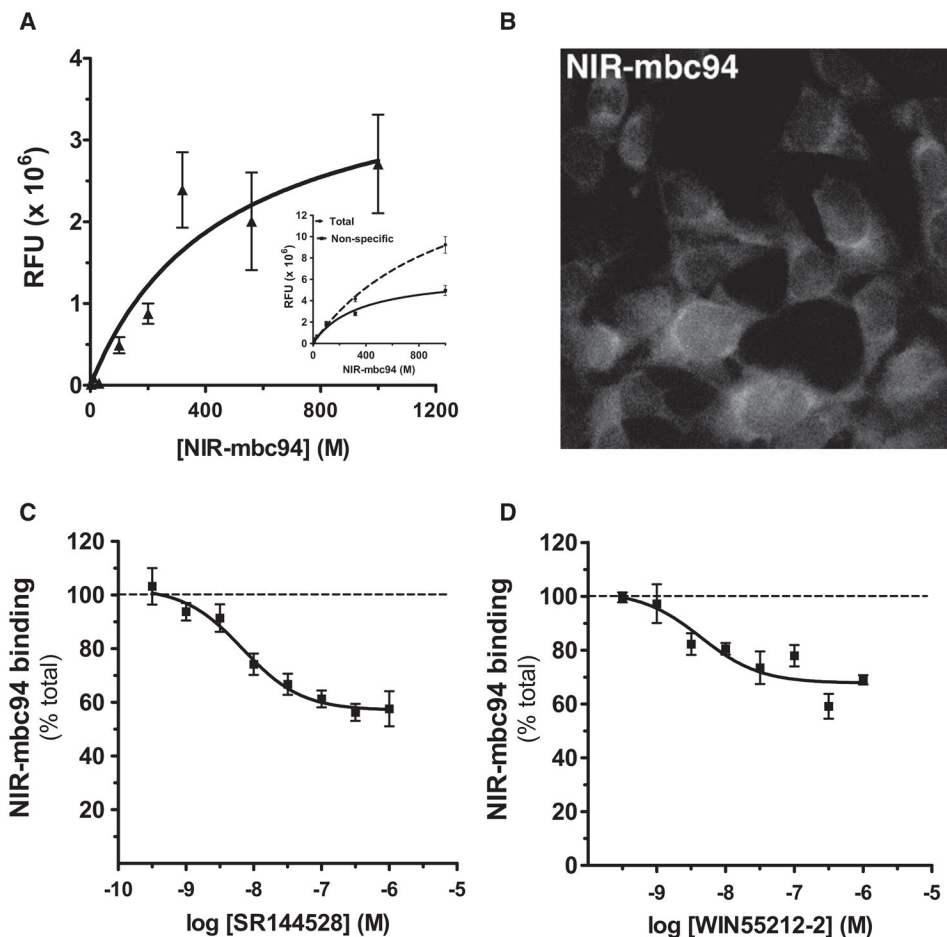
Figure 1. NIR-mbc94, a SR144528 Analog, Binds to CB$_2$ Receptors in Homogenates
(A) Chemical structure of SR144528. Shown are the three modification sites to which alkyl amino linkers were conjugated. Note that NIR-mbc94 was synthesized by conjugating the R3 position a carbon linker and IRDye 800CW, a NIR emitting fluorophore. For NIR-mbc94 structure, see Figure S1A.

(B) Radioligand binding competition curve of SR144528, mbc94 and NIR-mbc94. Experiments were performed using [^{3}H]-CP-55,940 (~3 nM) and homogenates prepared from CB$_2$ mid DBT cells. Specific binding is shown on y axis. Each data point represensts the mean ± SEM from three experiments, each performed in triplicate (using homogenates prepared from independent cell cultures).
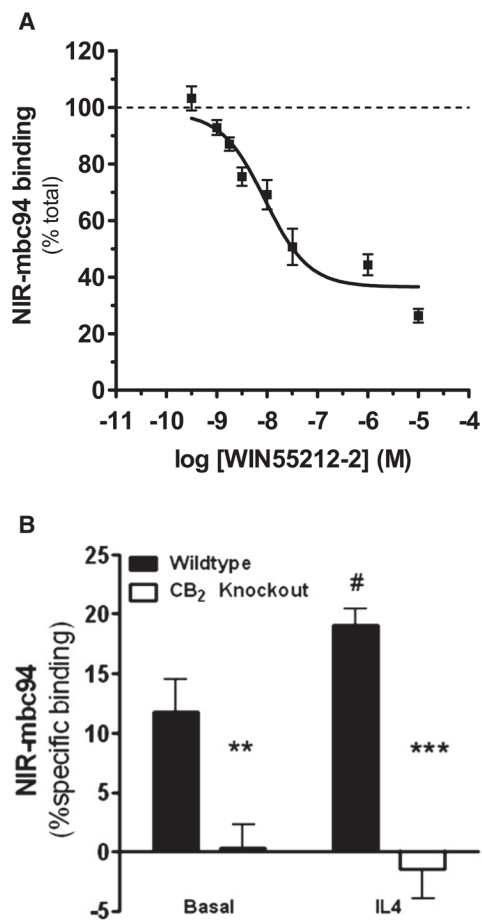
Figure 2. NIR-mbc94 Binds to CB$_2$ Receptors Expressed by Intact Cells: Heterologous Expression

(A) Saturation and competition of NIR-mbc94 binding to CB$_2$ receptors. Fluorescent signal emitted by increasing concentrations of NIR-mbc94 bound to CB$_2$ mid DBT cells was measured with a Li-Cor Odyssey scanner. Specific binding data are expressed as fluorescence values or relative functional units (RFU on the y axis) as a function of MI concentration (on the x axis). Data points for specific binding were obtained by subtracting the amount of fluorescence emitted by NIR-mbc94 incubated with CB$_2$ mid DBT cells minus fluorescence emitted by NIR-mbc94 incubated with untransfected DBT cells, using the values for corresponding concentrations. Inset shows these two curves. Data represent the mean ± SEM from three experiments, each performed in triplicate and on independent cell cultures.

(B) Image of NIR-mbc94 bound to CB$_2$ receptors. Shown is a representative image of NIR-mbc94 (1 μM) bound to CB$_2$ mid DBT cells, gated to the fluorescent signal emitted by NIR-mbc94 bound to untransfected DBT cells image (*i.e.* non-specific binding) (See Figure S2 for detailed images).

(C and D) Concentration-dependent competition of NIR-mbc94 bound to CB$_2$ receptors. CB$_2$ mid DBT cells were preincubated for 15 min with increasing concentrations of SR144528 (C) or WIN55212-2 (D), and then incubated for 30 min with NIR-mbc94 (200 nM). Fluorescence signal was measured with a Li-Cor Odyssey scanner. Data represent the mean ± SEM from at least three experiments, each performed in triplicate and on independent cell cultures.

See also Table S1.

A

B

Figure 3. NIR-mbc94 Binds to CB$_2$ Receptors Expressed by Intact Cells: Endogenous Expression

(A and B) NIR-mbc94 binds to CB$_2$ receptors expressed by (A) BV-2 cells and (B) mouse microglia in primary culture. Cells were preincubated for 15 min with either (A) increasing concentrations WIN55212-2 or (B), microglial cells from wild-type or CB$_2^{-/-}$ mouse pups were pretreated with or without IL-4 (10 ng/ml, 18 hr). Data represent the mean ± SEM of three experiments, each performed in triplicate and on independent cell cultures. **p < 0.01 and ***p < 0.001 significantly different from wild-type basal (one-way ANOVA); # p < 0.05 significantly different from wild-type basal (Students t test, two-tailed). See also Figure S3.